A high-throughput single-cell analysis of human CD8+ T cell functions reveals discordance for cytokine secretion and cytolysis

Navin Varadarajan,[1] Boris Julg,[2] Yvonne J. Yamanaka,[3] Huabiao Chen,[2,4] Adebola O. Ogunniyi,[1] Elizabeth McAndrew,[2] Lindsay C. Porter,[2] Alicja Piechocka-Trocha,[2,4] Brenna J. Hill,[5] Daniel C. Douek,[5] Florencia Pereyra,[2] Bruce D. Walker,[2,4] and J. Christopher Love[1,2,6]

[1]Department of Chemical Engineering, Massachusetts Institute of Technology, Cambridge, Massachusetts, USA. [2]The Ragon Institute of MGH, MIT, and Harvard, Boston, Massachusetts, USA. [3]Department of Biological Engineering, Massachusetts Institute of Technology, Cambridge, Massachusetts, USA. [4]Howard Hughes Medical Institute, Chevy Chase, Maryland, USA. [5]Human Immunology Section, Vaccine Research Center, National Institutes of Allergy and Infectious Diseases, NIH, Bethesda, Maryland, USA. [6]The Eli and Edythe L. Broad Institute, Cambridge, Massachusetts, USA.

CD8+ T cells are a key component of the adaptive immune response to viral infection. An inadequate CD8+ T cell response is thought to be partly responsible for the persistent chronic infection that arises following infection with HIV. It is therefore critical to identify ways to define what constitutes an adequate or inadequate response. IFN-γ production has been used as a measure of T cell function, but the relationship between cytokine production and the ability of a cell to lyse virus-infected cells is not clear. Moreover, the ability to assess multiple CD8+ T cell functions with single-cell resolution using freshly isolated blood samples, and subsequently to recover these cells for further functional analyses, has not been achieved. As described here, to address this need, we have developed a high-throughput, automated assay in 125-pl microwells to simultaneously evaluate the ability of thousands of individual CD8+ T cells from HIV-infected patients to mediate lysis and to produce cytokines. This concurrent, direct analysis enabled us to investigate the correlation between immediate cytotoxic activity and short-term cytokine secretion. The majority of in vivo primed, circulating HIV-specific CD8+ T cells were discordant for cytolysis and cytokine secretion, notably IFN-γ, when encountering cognate antigen presented on defined numbers of cells. Our approach should facilitate determination of signatures of functional variance among individual effector CD8+ T cells, including those from mucosal samples and those induced by vaccines.

Introduction

CD8+ CTLs are a prominent component of the adaptive immune response that contributes to the clearance of viruses in acute infection (1). Antigen-specific CD8+ T cells can exhibit a range of functions, including the production of effector cytokines, degranulation, cytolytic activity, suppression of viral replication, and proliferation upon exposure to cells presenting antigen (2–4). Poor or inadequate functional responses by effector CD8+ T cells, however, are at least partly responsible for persistent chronic infection by both HIV-1 and HCV (5, 6). The importance of CD8+ T cells for controlling replication in chronic human viral infections has motivated extensive research to define phenotypic and functional attributes of an effective response, and has perhaps been most extensively studied in the context of infection by HIV.

The production of multiple cytokines, the enhanced expression of a glycoprotein associated with degranulation (CD107a), and the combined ability to proliferate and produce perforin have all been partially correlated with improved viral control, but none is a robust surrogate for effective control (4, 7–11) or measures cell-mediated killing directly. Recent clinical trials of candidate vaccines for HIV, such as the Merck STEP trial, have shown that it is possible to induce HIV-specific CD8+ T cells, as measured by the ability to produce IFN-γ, determined by ELISpot and intracellular cytokine staining (ICS). Their presence, however, did not result in improved protection against infection or a reduction in the viral load set point after infection (12). The ability to monitor the efficacy of T cells raised in a natural infection or in response to a candidate vaccine, therefore, continues to be a central challenge (13).

The capacity of CD8+ T cells to lyse virally infected cells is a direct measure of an effective outcome but is not assessed by most immune assays currently in use (14). Assays that do assess bulk cytolytic activity are relatively insensitive for determining the activities of T cells ex vivo, and they do not assess the phenotypic qualities of the T cells themselves. To measure the responses from individual T cells in clinical studies, ELISpot is commonly used because it is easy to execute and validate, but the breadth of functions scored simultaneously has been limited (15). One variant on the ELISpot assay has been reported that provides a dual measure of the actual cytolytic capacity of CTLs ex vivo and the release of IFN-γ (16). The assay, however, is unable to detect cells that effect cytolysis without secreting IFN-γ, and because it relies on colorimetric indictors that are difficult to multiplex, it is also not well suited to examine the breadth of possible functional responses.

Authorship note: Navin Varadarajan and Boris Julg contributed equally to this work.

Conflict of interest: J. Christopher Love is a founder of and consultant for Enumeral Biomedical.

Citation for this article: *J Clin Invest.* 2011;121(11):4322–4331. doi:10.1172/JCI58653.

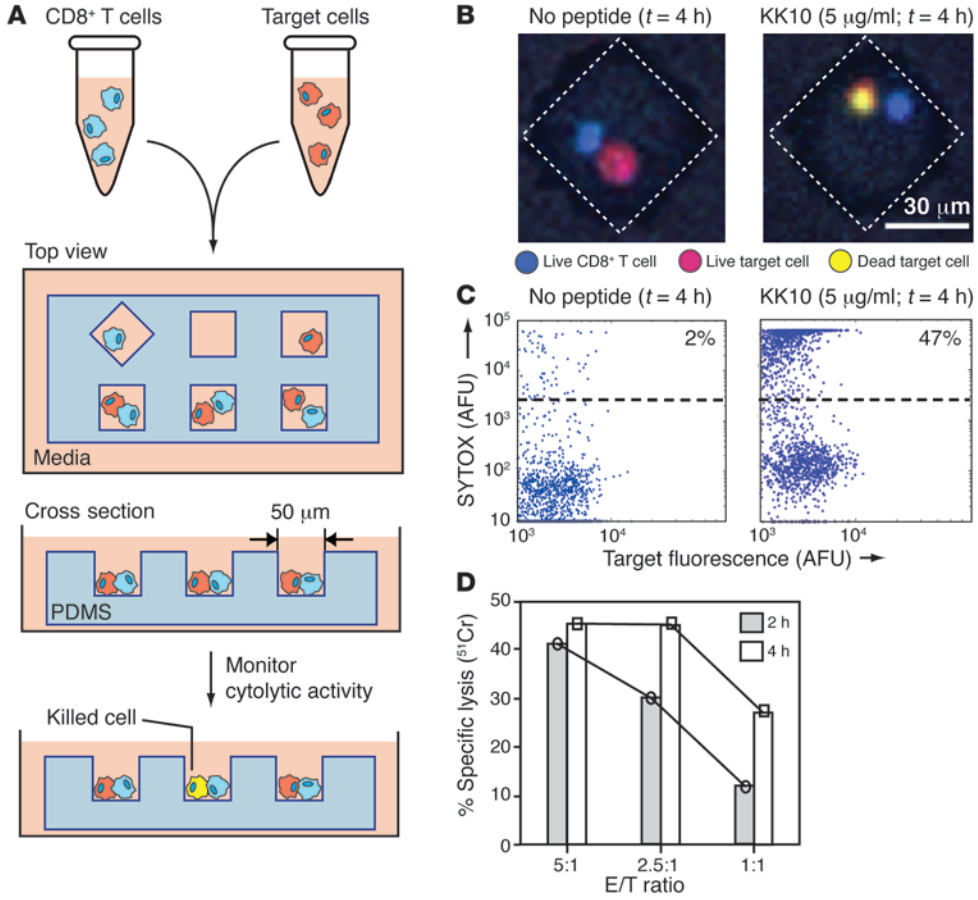

Figure 1

High-throughput, single-cell assay for cytolysis. (**A**) Schematic for the microwell-based assay. Unlabeled CD8+ T cells (blue) and labeled antigen-presenting target cells (red) are loaded sequentially onto an array, immersed in media, and then imaged at t = 0 hours and t = 4 hours. Dead target cells are identified by loss of integrity of the nuclear membrane (SYTOX, green; composite with CellTracker Red is superimposition of red and green (shown as yellow). (**B**) Representative composite micrographs of microwells containing individual KK10-specific CD8+ effector cells (clone E501) coincubated with naive or KK10-pulsed HLA-B*27+HLA-A*02+ B cells. Dashed lines indicate the perimeters of the wells. (**C**) Target cell scatter plots for wells containing 1 effector and 1 target at 4 hours without (left) and with (right) KK10; effectors not shown. For inclusion, targets in wells were gated as CellTracker Red positive (target fluorescence, $>10^3$) and SYTOX negative at 0 hours. Dashed line indicates the threshold for dead target cells, and the percentage is noted. AFU, arbitrary fluorescence units. (**D**) Plots of bulk cytolysis determined by ^{51}Cr release for KK10-pulsed B cells mediated by E501 after either 2 or 4 hours as a function of E/T.

ICS provides an alternative method to score multiple functions of antigen-specific T cells following activation in the presence of both high quantities of antigen and chemical treatments that inhibit secretion and prevent acidification (17). Despite its widespread use for determining associations of multifunctional responses by T cells with clinical diseases and responses to vaccines (18), ICS has three intrinsic limitations. First, it must rely on surrogate measures of cytolytic activity such as CD107a, since the associated target cells are lost during the assay. Degranulation is a general feature of antigen-experienced cells, and the ability of CD8+ T cells to induce target cell lysis appears more closely related to granule content than degranulation itself (19). A second limitation is that blocking secretion abolishes the ability to distinguish among intracellular, membrane-retained, and secreted forms of cytokines. For example, the membrane-bound form of TNF-α can effect cytolysis (20), but neither ICS nor surface capture with bispecific antibodies distinguish between that form and soluble protein. Third, the implementation of the assay — coincubation of hundreds of thousands of APCs with CD8+ T cells — makes it impossible to determine the sensitivity or responsiveness of individual T cells challenged with small numbers of APCs, as during natural infection.

Understanding the direct relationship between cytolysis and other functional responses by T cells, while preserving the ability to then further characterize specific reactive cells, should facilitate the determination of strongly correlated functions and monitoring of responses to vaccines (21). To investigate the relationship between cytolysis and the induction of secreted cytokines, we developed a high-throughput method that allows one to assess how in vivo primed individual HIV-specific CD8+ T cells respond upon encounter with a single cell presenting viral antigen. This approach for multidimensional single-cell analysis allows concurrent measures of both cytolytic activity and the secretion of cytokines. Using this new method, we present direct evidence that cytokine secretion by CD8+ T cells isolated ex vivo from HIV-infected patients — particularly IFN-γ — is largely independent of cytolytic activity. Only a small minority of cells exhibit both functions simultaneously; the majority of individual, functional antigen-specific cells either lyse target cells or secrete IFN-γ.

Results

Design and validation of a single-cell assay for antigen-specific cytolysis. We designed an assay to observe the cytolytic activity of individual CD8+ T effector cells encountering discrete numbers of peptide-loaded APCs as targets. The approach uses a dense, elastomeric array of wells with subnanoliter volumes (125 pl each) to execute thousands of independent single-cell cytolytic assays in parallel by coincubating T cells with APCs (Figure 1A). On-chip, live-cell cytometry using automated microscopy determines the occupancy of each of the approximately 85,000 wells in the array, and inclusion of a fluorescent, membrane-impermeant nucleic acid stain

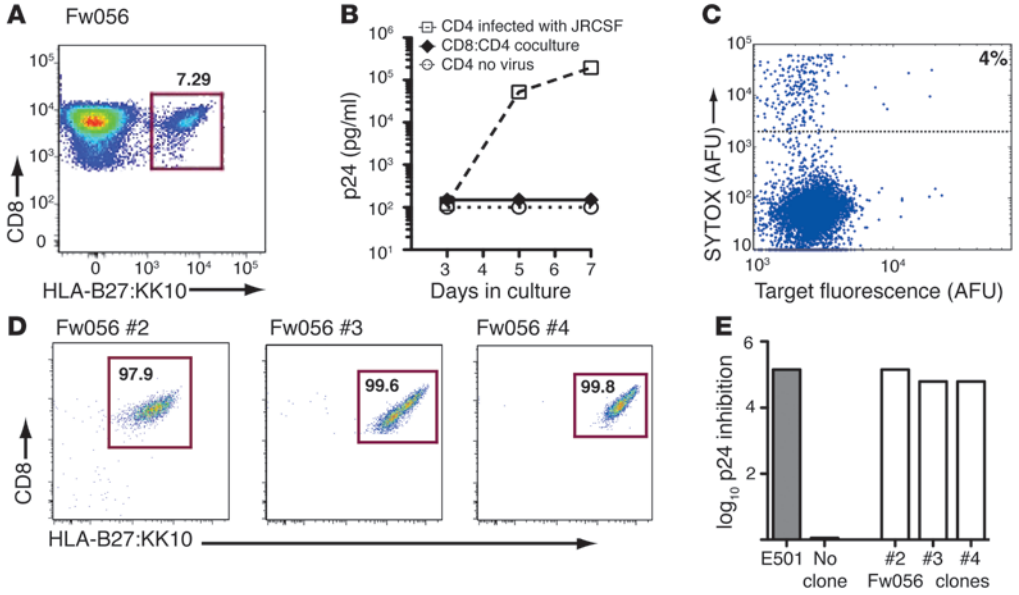

Figure 2

Ex vivo screening and recovery of HIV-specific cytotoxic effectors from clinical samples. (**A**) Scatter plot of the frequency of HLA-B*27-KK10–specific CD8+ T cells in an HIV+ elite controller (Fw056) determined by flow cytometry and staining with MHC class I tetramers. The percentages of gated populations are indicated. (**B**) Plot of the inhibited replication of HIV-1 in autologous CD4+ T cells mediated by ex vivo FACS-sorted KK10-specific CD8+ T cells from Fw056. The concentration of p24 was measured in the supernatants from cocultures of CD4+ T cells infected with a reference strain of HIV-1 (JRCSF) and autologous, isolated CD8+ T cells. Controls without CD8+ T cells and without infection are shown for reference. (**C**) Scatter plot of the percentage of dead (SYTOX) HLA-matched, KK10-loaded, labeled B cell targets observed in arrays of microwells following on-chip coincubation with ex vivo CD8+ T cells from Fw056 (E/T = 1:1–5:1). The dashed line indicates the threshold for dead cells. Shown are representative results from at least 4 independent measurements. (**D**) Scatter plots of HLA-B*27-KK10–specific CD8+ T cell clones (Fw056-2, Fw056-3, Fw056-4) identified based on observed cytolysis of target cells in microwells, retrieved by micromanipulation, and expanded in vitro. Epitope specificity was confirmed using MHC class I tetramers. (**E**) Plot of the inhibited replication of HIV-1 in HLA-matched CD4+ T cells mediated by the CD8+ T cell clones. Inhibition was determined in the same manner as in **B**, with supernatants collected at day 7. Controls with the CD8+ T cell clone E501 and without CD8+ T cells are shown for reference.

(SYTOX) in the media during incubation allows the dynamic assessment of cell death in permeabilized cells, since those that die become fluorescent (green).

To validate the assay, we deposited a CD8+ T cell clone specific for the HIV-1 p24 Gag epitope KK10 (E501), restricted by HLA-B*27, into the wells of the array. Application of 300 μl containing 1.5×10^5 cells to the array yielded a distribution of approximately 1 cell per well. To minimize perturbations to the functional activity of the T cells, we did not label these cells at the time of deposition. For APCs, we used HLA-matched, EBV-transformed B cells, because as a population, they exhibited a consistent phenotype (expressing CD11c, CD70, and CD80, but not CD11b, CD83, or CD86) and thus also provided consistency in antigen presentation to facilitate comparisons among T cells in different microwells on the array and among populations of T cells derived from different subjects. (Such lines can also be generated in clinical studies to allow autologous antigen presentation; ref. 22.) The B cells were labeled with a cytosolic dye (CellTracker Red) to identify metabolically active live cells, pulsed for 60 minutes with the cognate CTL epitope targeted by this clone, and then washed. A suspension of these cells was subsequently loaded onto the array of wells containing the effector cells. This two-step process for loading wells with both types of cells typically yielded 3×10^3 to 6×10^3 microwells containing exactly one effector and one target cell, with approximately 10^4 wells containing at least one effector and a single target (Supplemental Figure 1; supplemental material available online with this article; doi:10.1172/JCI58653DS1). The APCs were pulsed with a high dose of the peptide to promote uniform presentation by each individual APC, but excess antigen was removed by washing the cells prior to their deposition onto the array. In this way, the number of target cells in each well defined the maximum dose of antigen to which co-loaded T cells could be exposed.

After the array was loaded with both target and effector cells, it was immersed in media containing SYTOX and imaged to determine cell viability. Wells containing dead target cells at the start of the assay (SYTOX-positive) were excluded from further analysis. Arrays were incubated for 4 hours, followed by in situ labeling of cells with a live-cell stain (calcein violet), and imaged again. These images were used to determine the number of viable T cells (blue), plus the numbers of viable (red) and dead (red + green) targets, in each well.

Automated quantitative analysis of more than 5,000 independent T cell–APC interactions per experiment was performed to determine the specificity of lysis by E501 cells incubated with target APCs with or without the cognate KK10 epitope (Figure 1, B and C). Wells containing E501 effector cells coincubated with KK10-loaded APCs showed increased numbers of dead target cells over 4 hours (29%–47%). In the absence of this peptide, the number of dead APCs observed in wells containing E501 cells after 4 hours was 2%–3%, which was comparable to the typical frequency of spontaneous death observed in wells containing only APCs (Supplemental Figure 2). Time-lapse video microscopy on loaded arrays confirmed that the effector cells were highly mobile in the wells during the period of incubation, typically engaging target APCs within an hour of loading and subsequently permeabilizing the membranes of cells pulsed with matched peptide (Supplemental Video 1). These single-cell data were consistent with the specific lysis observed after 4 hours using the same populations of effector and target cells in a ^{51}Cr release assay (27%–45%, Figure 1D).

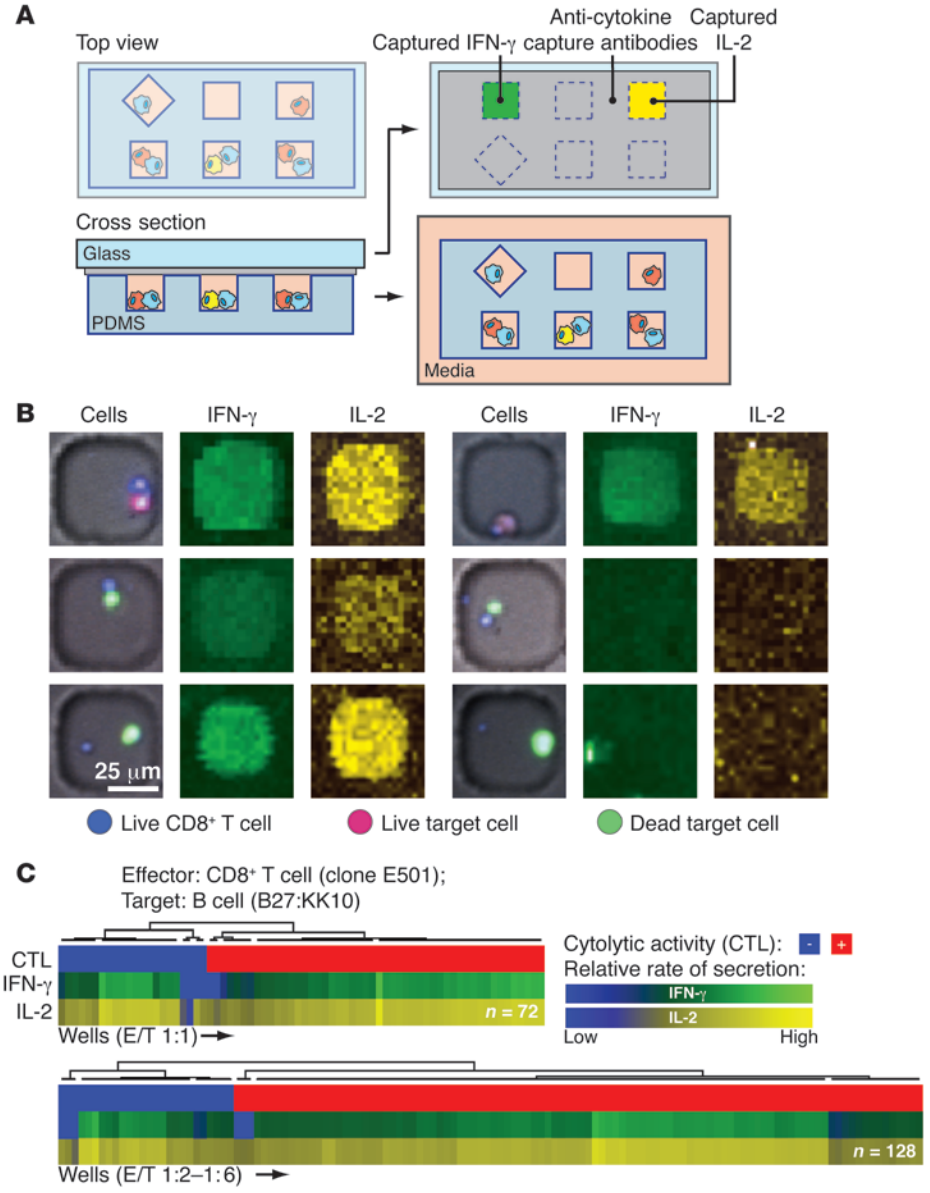

Figure 3
Integrated single-cell analysis of immediate cytotoxicity and short-term cytokine secretion from T cell clones. (**A**) Illustration of the assay for concurrent detection of cytolytic activity and secretion of cytokines. Following incubation of targets and effectors in microwells, the array is contacted with a glass slide bearing cytokine-specific antibodies to capture multiple secreted cytokines per well (IFN-γ, IL-2, and TNF-α). The resulting microarray of cytokines is labeled and matched to the array of microwells to correlate cytolysis with secretion of cytokines. (**B**) Representative composite micrographs of cytolytic activity (or lack thereof) in wells containing single effectors (E501) and single targets (EBV-transformed B cell) after coincubation for 4 hours and matching fluorescence micrographs of corresponding captured cytokines on the microengraved array. Scale bar: 25 μm. (**C**) Matched data for concurrent measurement of cytolysis and IFN-γ/IL-2 secretion for single E501 $CD8^+$ T cells ($n = 200$). The wells are segregated according to the number of targets in each well: E/T = 1:1 ($n = 72$) (top) and E/T = 1:2–1:6 ($n = 128$) (bottom). The data are shown as a heatmap and organized by unsupervised hierarchical clustering (Euclidean distance, complete linkage). Cytolytic activity is shown as discrete values. The relative rates of secretion are shown for IFN-γ (green) and IL-2 (yellow). Dendrograms indicate the relative calculated distances among clusters of wells. No E501 cells released TNF-α at a detectable rate (>~2 molecules/s). The number of cytolytic events with T = 1 was not significantly different from those with T >1 ($P = 0.17$, 2-tailed Fisher's exact test).

Effector-mediated lysis was confirmed to be specific to the cognate epitope in a crossover experiment. B cells were pulsed with either KK10 or a different Gag epitope, SL9 (1 μg/ml), and then loaded into microwells containing $CD8^+$ T cell clones specific to either KK10 (clone E501) or SL9 (clone A14) (minimum $n = 2{,}924$ per experiment). Effector-mediated lysis was 29%–44% when matched peptides were used (E501 clones with KK10-pulsed targets; A14 clones with SL9-pulsed targets), but less than 1% when T cell clones were coincubated with B cells loaded with irrelevant peptides (E501 clones with SL9-pulsed targets; A14 clones with KK10-pulsed targets). Together, these experiments using T cell clones demonstrated the feasibility of measuring HIV-specific cytolytic activity by on-chip cytometry for many thousands of independent events in parallel in spatially defined arrays of microwells.

Detection of HIV-specific cytotoxic effector T cells from clinical samples. These experiments with T cell clones suggested that it should be possible to detect HIV-specific $CD8^+$ T cells from clinical samples based on their cytolytic activity. To examine this hypothesis, we identified a subject who controls HIV spontaneously and has a robust response to the same B*27-restricted Gag KK10 epitope targeted by the clone. Approximately 7%–8% of circulating $CD8^+$ T cells from peripheral blood were KK10 specific by MHC class I tetramer staining (Figure 2A). Analysis by flow cytometry indicated that the population of KK10-specific $CD8^+$ T cells comprised a range of differentiated states (predominantly T_{EM}, T_{EMRA}, and T_{CM}, where EM indicates effector memory; EMRA, effector memory RA; and CM, central memory) (Supplemental Figure 3). This population of cells reduced viral replication of an HIV laboratory strain in vitro using a viral suppression assay measuring released p24 (Figure 2B), with a smaller percentage of antigen-dependent responses detected by IFN-γ ELISpot (2,277 SFU/10^6 PBMCs).

For direct assessment of cytolytic activity, $CD8^+$ T cells were isolated from previously frozen PBMCs by negative enrichment with antibody-coated magnetic beads and coincubated with labeled,

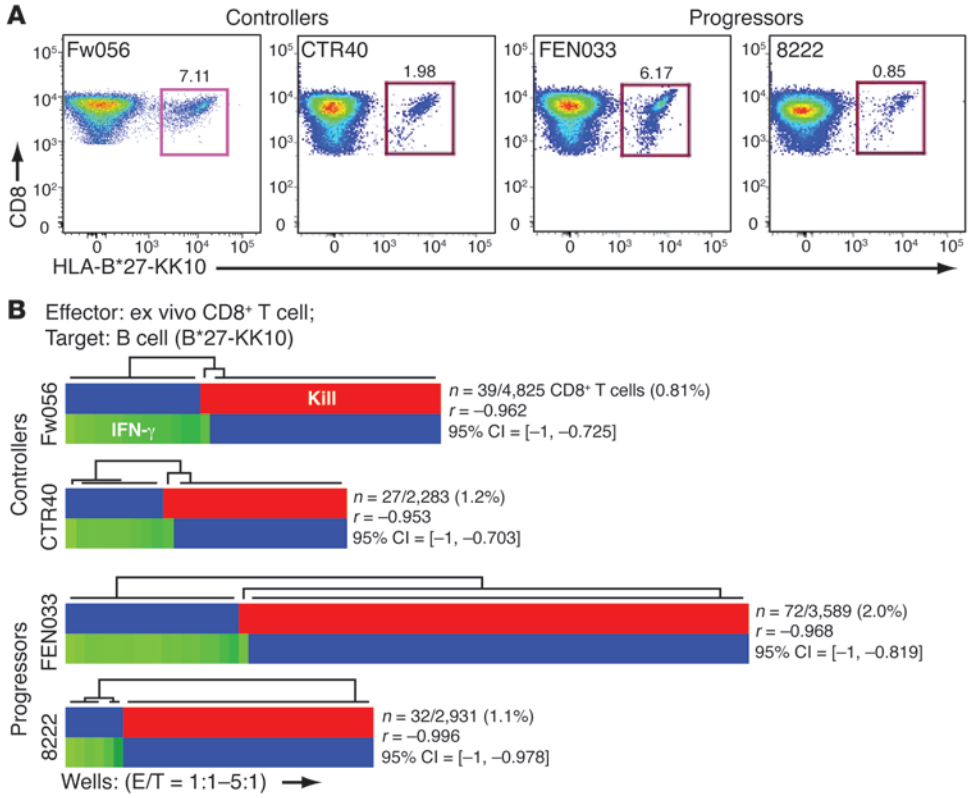

Figure 4

Direct evidence that immediate cytotoxicity and short-term IFN-γ secretion are not correlated functions for ex vivo HIV-specific CD8+ T cells. (**A**) Representative scatter plots of the frequencies of HLA-B*27-KK10–specific CD8+ T cells in 4 different clinical samples (2 elite controllers [Fw056, CTR40] and 2 progressors [FEN033, 8222]) determined by flow cytometry and staining with recombinant MHC class I tetramers. The percentages of gated populations are indicated. (**B**) Matched data for concurrent measurement of cytolysis and IFN-γ secretion for ex vivo CD8+ T cells from 4 HIV+ individuals coincubated in arrays of microwells for 6 hours with single HLA-matched, KK10-pulsed target B cells. The data are shown as a heatmap and organized by unsupervised hierarchical clustering (Euclidean distance, complete linkage). Cytolytic activity is shown as discrete values (blue, negative; red, death). The relative rate of secretion is shown for IFN-γ (green). The dendrograms indicate the relative calculated distances and separation among clusters of wells. All events with any functional activity are shown; the total number of CD8+ T cells in wells with E/T = 1:1–5:1 is indicated for each sample. There were no cells among any of the 4 samples that released either IL-2 or TNF-α at a detectable rate (limit of detection, ~2 molecules/s). The Pearson's product-moment correlation coefficient (*r*) and 95% CI were estimated for each dataset by random data resampling. The data are representative of at least 3 independent measurements for each subject.

peptide-pulsed (B*27-KK10, 5 μg/ml), HLA-matched B cell targets in arrays of microwells in the same manner as described above. After incubation for 6 hours, target cell death was identified based on SYTOX staining (Figure 2C). Antigen-dependent cell lysis was reproducibly detected in wells containing both T cells and target cells with cognate peptide (136 of 3,029 events; 4.5%), whereas the number of target cells spontaneously dying on-chip was only 66 of 2,485 (2.7%). The small antigen-dependent difference measured was statistically significant (Fisher's exact test, $P = 0.0003$) and reproducible in 4 independent replicates of the experiment. The number of dead cells observed when target cells presented an irrelevant melanoma epitope was not different from spontaneous deaths (108 of 3,864; 2.8%, $P = 0.90$).

To verify further the antigenic specificity of the identified CTLs, individual cells that mediated killing in the assay were then retrieved by micromanipulation and seeded into 96-well plates containing irradiated HIV-uninfected PBMCs for clonal expansion (23). Although not all of these cells could be propagated in culture, 3 of 3 successfully expanded cytolytic CD8+ T cells from the microwell array were highly specific for the KK10 epitope, as determined by MHC class I tetramer staining (Figure 2D). CD8+ T cells randomly selected from wells without targets proliferated robustly, but none were antigen specific, as expected given the frequency of antigen-specific cells in the CD8+ T cell population. The limited efficiency of expansion among the cytolytic effector T cells likely indicates that the majority of cytolytic events measured result either from cells with a terminally differentiated phenotype that cannot expand or from cells that subsequently die due to activation-induced cell death (24, 25).

Sequence analysis of the T cell receptors from all three recovered antigen-specific clones showed distinct differences in Vα and Vβ chains (Supplemental Table 1). These clones also exhibited robust antiviral activity (10,000- to 100,000-fold reduction in measured p24 on day 7) in a viral suppression assay that measured their ability to inhibit replication of an HIV-1 laboratory strain (JRCSF) in activated, HLA-matched CD4+ T cells (Figure 2E). This result was similar to the antiviral activity that had been observed using tetramer-based sorting of KK10-specific CD8+ T cells from peripheral blood of this person (Figure 2B). These results show that the microwell assay can detect individual, antigen-specific cytolytic effector cells within peripheral blood and that a diversity of clonotypes is primed for rapid cytolysis within the subset of T cells that label with MHC I tetramers.

Integrated measure of short-term cytokine secretion and immediate cytotoxicity. The production of IFN-γ has been used as an assumed surrogate for HIV-specific cytolytic activity during the progression of disease and to assess the immunogenicity of candidate vaccines. In the absence of a direct assay to measure both functions (cytolysis and secretion), it has remained unclear to what extent cells exhibit both responses concurrently when encountering an APC. We have previously shown that the elastomeric array of microwells used here can also detect the frequencies and rates of secretion of multiple cytokines by a process called microengraving (26, 27). According to this method, a glass slide coated with antibodies specific for

cytokines of interest is used to seal the microwells, and thereby confines the cells to the subnanoliter volumes of the microwells. After a short incubation (1–2 hours), the glass is removed to yield an array of cytokines registered to the array of microwells. Using this method, we have demonstrated, and confirmed with quantitative models, the ability to measure the secretion of IFN-γ, IL-2, and TNF-α simultaneously from polyclonally activated, primary T cells ex vivo with sensitivities 10- to 100-fold greater than ELISpot and surface-based capture (27).

We integrated the single-cell cytolytic assay described here with microengraving to measure the relationship between cytokine release and cell killing by individual antigen-specific $CD8^+$ T cells when encountering one or a small number of APCs (Figure 3A). To first validate this integrated assay, fluorescently labeled, peptide-pulsed (B*27-KK10, 5 μg/ml) B cell targets were coincubated with unlabeled E501 effectors in arrays of microwells, in the presence of costimulatory antibodies (αCD28 and αCD49d) to further minimize heterogeneity in antigen presentation among the APCs. After incubation for 4 hours, effector-mediated lysis was identified by image-based cytometry. The array of microwells was then rinsed with serum-free medium and placed in contact with a glass slide bearing antibodies specific for IFN-γ, IL-2, and TNF-α. Following incubation for an additional 2 hours at 37°C, the glass slide was removed, labeled with fluorescent antibodies, and imaged to determine wells that contained cells secreting cytokines (Figure 3B).

The majority of the clonal E501 cells exhibited lytic activity and secreted both IFN-γ and IL-2, but not TNF-α (Figure 3C). For various ratios of effectors to targets (E/T = 1:1–1:6), 67%–76% of effectors secreted both IFN-γ and IL-2 and lysed their target-cells; 3% secreted only IL-2 and induced lysis. Target cells lacking antigen and coincubated with E501 effectors showed 1%–2% spontaneous lysis, with no detectable cytokine secretion, confirming that the release of these cytokines depends on antigen-specific recognition. This combined assay, therefore, enables direct monitoring of both antigen-induced cytotoxicity and secretion of cytokines for individual effector cells, and shows that an IL-2–dependent HIV-specific CTL clone propagated in vitro can express dual functions of cytokine secretion and cell killing.

Immediate cytotoxicity by circulating HIV-specific $CD8^+$ T cells does not correlate with short-term IFN-γ secretion. The validation of the assay to measure cytolytic activity and antigen-induced secretion of cytokines concurrently, in combination with the successful measurements of ex vivo cytolysis by CTL clones from an HIV-infected patient, allowed us to next address the relationship between immediate cytolytic activity and secretion of IFN-γ by circulating HIV-specific $CD8^+$ T cells. We selected 4 HIV-infected patients, 2 with spontaneous control of infection and 2 with chronic viremic disease, who each exhibited robust HIV-specific responses for the KK10-epitope (range [0.85%, 7.11%]) in their bulk $CD8^+$ T cell populations, as measured by tetramer staining (Figure 4A). We isolated $CD8^+$ T cells by negative selection from frozen samples of PBMCs from each patient, and coincubated them in arrays of microwells with fluorescently labeled, HLA-matched, KK10 peptide–pulsed B cell targets. Immediate cytotoxicity was scored by imaging the arrays after 6 hours, and the secretion of cytokines (IFN-γ, IL-2, and TNF-α) was determined by microengraving during the final 2 hours of the assay. The data for cytotoxicity and cytokine release were then correlated for each well and segregated based on the number of targets per well (1 or 2–6). The number of effector cells was allowed to range from 1 to 5 because the probability of multiple antigen-specific T cells being confined in a single well is low, and the mean occupancy of T cells per well was between 1 and 2 for each sample. (When antigen-specific cells constitute 5% of the population, statistically 9.5% of wells with two $CD8^+$ T cells will contain a single antigen-specific cell, whereas both cells will be antigen-specific in only 0.25% of the wells. Thus, any observed function in a well with two effector cells is 38 times more likely to result from a single antigen-specific cell than from two.) After filtering the matched data to remove wells with targets that were dead at the initial time point (t = 0 hours), approximately 2,000–3,000 independent events per sample were identified containing effectors coincubated with single targets (E/T = 1:1–5:1).

Finally, we also incubated the same B cell lines with ex vivo $CD8^+$ T cells from all 4 patients, but without exogenous or irrelevant peptides, in order to verify that endogenous peptides presented by the EBV-transformed B cell lines did not induce confounding $CD8^+$ T cell responses. In these experiments, the numbers of cytolytic events observed were indistinguishable from the number of spontaneous deaths of target cells from wells on the same arrays containing no T cells ($P \geq 0.90$). These arrays also yielded fewer than 1 IFN-γ^+ event per 5,000 wells (<0.02%) by microengraving. These data confirmed that processing and presentation of endogenous peptides by the target cells did not significantly affect the detection and quantification of HIV-specific $CD8^+$ T cell responses for these subjects.

The frequency of HIV-specific IFN-γ^+ $CD8^+$ T cells from each subject determined by microengraving ranged from 0.6% to 0.9%. This result was comparable to the frequency of IFN-γ^+ cells as measured by standard ELISpot upon stimulation with KK10 peptide ([0.12%, 0.38%]) (Supplemental Figure 4). Since both our assay and ELISpot measured frequencies of IFN-γ^+ events that were smaller than the fraction of tetramer-positive T cells determined by flow cytometry, we also assessed the KK10-specific intracellular production of IFN-γ in PBMCs from all 4 patients by flow cytometry (Supplemental Figure 5). These data showed that a number of cells produced IFN-γ in an antigen-dependent manner, but not all of them labeled with tetramers, and that the total number of tetramer-positive events following antigenic exposure was less than that in the absence of peptide. These results further suggest that antigen-dependent functional responses do not necessarily correspond with tetramer labeling.

The number of effector cells mediating cytotoxicity in our assay ranged between 0.5% and 1.9% of $CD8^+$ T cells and was comparable among all 4 subjects. Correlation of IFN-γ secretion and cytolytic activity for individual effector cells, however, indicated that reactive, antigen-specific $CD8^+$ T cells encountering a single APC either released IFN-γ or lysed their targets (single function, [0.8, 2.0%]), but rarely mediated both functions (dual function, [0, 0.04%]) (Figure 4B). We applied 4 different statistical analyses to test the hypothesis resulting from our data that cytolytic activity and IFN-γ secretion occur discordantly. First, a randomized resampling analysis was used to estimate the correlation coefficient for IFN-γ secretion and cytotoxicity. All functional events detected in the wells provided a common pool from which a subset of events was drawn 50,000 times; the number of events in each subset was based on the expected number of antigen-specific events relative to spontaneous death or nonspecific cytokine release on the array. This test showed a strong anti-correlation between cytolysis and secretion ($r < -0.95$ for each subject) (Figure 4B). Second, we applied the hypergeometric dis-

tribution to test the significance of overlap in cytolytic activity and IFN-γ secretion. Using the number of dual function events observed from each sample (n_{dual}), we calculated the probability that at least n_{dual} events would be observed due to random overlap between cytolytic activity and secretion. For all samples, this probability was greater than 0.05, suggesting that none of the samples had significant overlap in cytolytic and IFN-γ secretion functionality. Third, we calculated the probability (P) that the rare events with dual functions resulted from the random overlap of the secretion of IFN-γ and spontaneous death of the target cell. For each subject, we found $P > 0.3$, further indicating that there is not a significant overlap between cytolytic and secretion behavior in individual effector cells. Finally, we analyzed wells with 1–5 effectors and more than one target. These data confirmed that few $CD8^+$ T cells exhibited both functional activities concurrently ([0.17, 0.37%]) (Supplemental Figure 6). The number of IFN-γ^+ cells that exhibited cytolytic activity did not increase significantly for any of the subjects with $T > 1$ ($P > 0.4$).

The magnitude and breadth of functional $CD8^+$ T cell responses have been shown to depend on the concentration of antigen to which the cells are exposed (28, 29). We therefore performed a peptide titration experiment by integrated single-cell analysis using $CD8^+$ T cells isolated from one of the elite controllers (Fw056) coincubated with B cell targets that were pulsed with a range of concentrations of KK10 peptide. For peptide concentrations greater than or equal to 500 ng/ml, the frequencies of cytolytic events were significantly greater than in the control ($P < 0.01$; Fisher's exact test, or, for large numbers of events, χ^2 with Yate's correction) and increased with concentration (Supplemental Figure 7A). All 3 non-zero concentrations of peptide (50 ng/ml, 500 ng/ml, 5 μg/ml) induced a consistent percentage of cells secreting IFN-γ ([0.49, 0.64%]), with the relative rates of secretion significantly higher for concentrations of 500 ng/ml and 5 μg/ml relative to that at 50 ng/ml (Supplemental Figure 7B). No such secretion events were scored in the absence of peptide, confirming a low rate of false-positive responses for secretion of IFN-γ with only endogenous peptide. The overlap of the cytokine secretion with cytolytic activity remained minimal.

To further investigate the relationship between HIV-specific cytotoxicity and IFN-γ secretion, we next conducted the combined assay for 2 patients with an alternate, robust $CD8^+$ T cell response to A*02-SL9. Similar to the KK10-specific response, we found that SL9-specific $CD8^+$ T cells showed moderate IFN-γ responses (0.4% and 0.5%). The frequency of $CD8^+$ T cells capable of both cytolysis and IFN-γ secretion was again low (0.06% and 0.07%, Supplemental Figure 8).

The above studies indicate the ability to assess the functions of effector cells when the targeted epitope is known. To determine whether this assay might be useful when the cognate epitope is not known, we loaded the array of microwells with B cell targets (EBV transformed; derived from an HIV-infected subject) that had been pulsed with a pool of overlapping peptides spanning the entire Gag protein. We then added autologous $CD8^+$ T cells and examined the antigen-specific dual functionality of these cells. Discordant responses were again observed, without requiring a priori knowledge of the epitopes targeted or the restricting HLA alleles. In wells with 1–5 effectors and a single target, 0.29% of the $CD8^+$ T cells secreted IFN-γ and 0.95% lysed their target, but no effector cells were observed to both secrete IFN-γ and lyse a target (Supplemental Figure 9). Together, these data provide direct evidence that cytolysis can occur independently of secretion of IFN-γ and that this segregation of functional responses is not restricted to a particular epitope.

Discussion

We present here a high-throughput single-cell assay to directly observe cytolytic activity and cytokine secretion ex vivo. Using this integrated approach to functional analysis, we found that when circulating antigen-specific $CD8^+$ T cells isolated from persons in the chronic phase of HIV infection engage a single APC, they predominantly exhibit either the secretion of IFN-γ or cytolytic activity, but infrequently exhibit both functions simultaneously. This assay provides a new tool for evaluating multiple functional activities associated with antigen-specific primary T cells following encounter with one or a small number of APCs and importantly, for the first time to our knowledge, allows the retrieval, expansion, and additional in vitro characterization of single effector cells based directly on their ability to lyse a target cell.

Our validation of the cytolytic assay using microwells focused primarily on two epitopes found in Gag: HLA-B*27–restricted KK10 and HLA-A*02–restricted SL9. The nature of the functional responses observed among the 4 patients with high frequencies of KK10-specific T cells (as determined by flow cytometry) was similar with respect to both outcome (cytolysis and/or IFN-γ secretion) and magnitude of functional activities (~1% of $CD8^+$ T cells). Genome-wide association studies have indicated that HLA-B*27 is a protective allele associated with slow disease progression and low plasma viral loads (30), and several studies have suggested that HLA-B27–positive patients infected with HIV clade B mount an immunodominant response to KK10 (31, 32). $CD8^+$ T cells restricted by HLA-B*27-KK10 are also known to effectively inhibit replication of HIV in vitro (33). Thus, despite the differences in viral loads, it is perhaps not surprising that $CD8^+$ T cells from the chronic viremic subjects targeting this highly conserved epitope would exhibit cytolytic activity in vitro that is as robust as those from the controllers. The differences in in vivo viral loads may also indicate the presence of viral escape mutants (34).

The lysis of individual targets by individual antigen-specific effectors may simply eliminate cognate antigenic stimulation before a sufficient level of signal is transduced to initiate the release of one or more cytokines. Measurements of cytolytic activity and IFN-γ by bulk assays using CTLs from perforin-deficient mice support this conclusion that the loss of TCR-mediated stimulation may limit the subsequent release of cytokines (35). Interestingly, the majority of $CD8^+$ T cells that did secrete IFN-γ upon stimulation with small numbers of APCs in our assay did not exhibit concurrent cytotoxicity, indicating that these functions are independently regulated.

Additionally, for ex vivo T cells exposed to a limited number of APCs, there was no significant secretion of TNF-α or IL-2. The paracrine release of detectable quantities of either IL-2 or TNF-α may require prolonged antigenic stimulation beyond the time allowed in these assays or require engagement with large numbers of target cells or quantities of antigen. Our data are consistent with a previous analysis of the sensitivity of ex vivo HIV-infected $CD8^+$ T cells to the concentration of antigen. In that analysis, systematic titration of antigen (peptide) showed that cytotoxicity (measured indirectly using CD107a) and production of IFN-γ required only low concentrations of antigen relative to the concentrations necessary to induce TNF-α and IL-2 (28). In our approach, target cells pulsed with anti-

gen prior to their deposition onto the array provide a defined in vitro experimental configuration that limits the total quantity of antigen to which T cells are exposed. In this way, the assay allows a combined measure of both multifunctionality and sensitivity ex vivo.

The ability to measure cytolytic activity directly, in combination with other functional responses, should provide a useful new tool to map the correlative relationships between cytolysis and potential surrogates for the efficacy of the response induced among T cells during infections or vaccinations. Antigen-specific $CD8^+$ T cells are commonly enumerated using recombinant multimers of MHC-peptide complexes, but as evident here, and reported by others (36, 37), there can be discrepancies between the numbers of labeled cells (quantity) and functionally active ones (quality). Low avidity between TCRs and the multimeric complexes may also affect the numbers of antigen-specific cells counted. Indeed, clonotypic variants specific for the same epitopes within a subject can have a range of avidities, and these differences affect their diversity of functional responses (38). Our method minimizes the bias required to select populations of T cells tested. That is, it does not require selecting on the ability to bind complexes of peptides and MHC prior to assessing functional response and thus allows the characterization of T cells with TCRs of low avidities that may be discounted in characterization by flow cytometry.

This new technique should also facilitate the enumeration of unique subsets of cells induced in natural infections that have noncanonical states of differentiation or lineages but potent functional responses (39). One specific advantage gained by using microfabricated systems for these analyses is that the number of cells required is small and is, therefore, conducive to evaluating mucosal samples or other clinical samples with limited numbers of cells (e.g., pediatric samples). One disadvantage of the demonstrated assay in the current format is that it employs EBV-transformed B cells as targets. Although we found that the endogenous presentation of antigens by these cells did not result in cytolysis rates that differed significantly from nonspecific cell death, the frequencies of EBV-specific $CD8^+$ T cells in a given sample could contribute to the lower limit of detection for cytolytic events by increasing the background number of events. This degree of sensitivity may constrain the individual analysis of less-abundant antigen-specific variants. This challenge could be addressed by using pooled peptides encompassing entire viral proteomes or whole immunogens to induce a high frequency of response, or defined, transfected cell lines presenting specific HLA alleles.

Future advances to incorporate autologous APCs, including infected cells, and other mechanism-dependent markers for cytolysis (e.g., caspase activation) would further enhance the utility of this tool. Expanding the breadth of parameters scored per assay using advanced imaging modalities or alternative labeling strategies would also improve the resolution of phenotypic variations measured. Nonetheless, our findings highlight the importance of developing high-throughput technologies for dynamic, multidimensional analysis of single T cells isolated ex vivo in a manner that allows direct correlations of functional responses under conditions of defined antigen stimulation. They also suggest that alternative approaches for routine, dynamic monitoring of the functional profiles of CTLs induced by novel vaccines for HIV or other diseases are possible.

Methods

Study subjects. Three HIV elite controllers with plasma HIV RNA levels of less than 50 copies/ml plasma in the absence of antiretroviral therapy were selected from the International HIV Controllers Study (http://www.hivcontrollers.org) (30). Two untreated viremic progressors with plasma HIV RNA levels greater than 2,000 copies/ml (HIV plasma RNA: median, 3,692 copies/ml; range 189–34,172) were recruited from outpatient clinics at local Boston hospitals. Patients were selected based on HLA-B*27 expression and strong $CD8^+$ T cell responses directed against the KK10 epitope in Gag, as assessed by IFN-γ ELISpot. None of the subjects were on antiretroviral therapy.

Microwell cytolysis assay. All dyes were purchased from Invitrogen, and all antibodies were purchased from BD. The array of microwells was fabricated by replica molding as described previously (27). The array was oxidized by exposure to an oxygen plasma for 30 seconds (Harrick PDG-32C) to sterilize the array and render the surface hydrophilic. A suspension (1.5×10^5 cells, 300 μl) of $CD8^+$ T cells was then placed on the surface of the array, and the cells were allowed to settle by gravity for 10 minutes. After a brief wash, a suspension (1.5×10^5 cells, 300 μl) of fluorescently labeled (CellTracker Red, 2 μM for 15 minutes) B cells, preloaded with either HIV-1 peptide KK10 or SL9 (5 μg/ml, 60–90 minutes), a pool of overlapping peptides spanning the HIV-1 Gag protein (2 μg/ml), or the melanoma peptide EV9 (1–5 μg/ml). The array was subsequently washed with RPMI 1640 complete medium supplemented with 10% FBS (R10) to rinse away cells not isolated in wells. The loaded microarray was then immersed in R10 containing 500 nM SYTOX dye (T cell medium) and left in the incubator (37°C, 5% CO_2) for 15 minutes. An initial set of fluorescence images (t = 0 hours) of the loaded microwell array was collected on an automated epifluorescence microscope (Zeiss). After imaging, the array was incubated for 3.5 hours (for experiments with T cell clones) or 5.5 hours (for experiments with primary $CD8^+$ T cells) at 37°C, 5% CO_2. A 1-μM (500 μl) solution of calcein violet in T cell medium was then added to the surface of the array (20 minutes), and a second set of images of the array (t = 4 hours [T cell clones] or t = 6 hours [primary $CD8^+$ T cells]) was recorded on the microscope.

Combined microwell cytolysis and multiplexed cytokine secretion assay. In order to be able to monitor the concurrent cytolysis and cytokine secretion of $CD8^+$ T cells, we combined the microwell cytolysis assay described above with the previously reported microengraving assay (27, 40). The initial microwell cytolysis assay was performed exactly as described above, except that costimulatory antibodies, anti-CD28 and anti-CD49d (1 μg/ml each), were included as part of the T cell medium. After acquiring the second set of images on the microscope, the array was washed with serum-free medium containing 5 ng/ml IgG (to facilitate registration of the microwell array to the printed microarray). A poly-lysine functionalized glass was preincubated with capture antibodies against IFN-γ, TNF-α, IL-2, and Ig (25 μg/ml each, 1 hour). The slide was blocked with 3% milk/PBS-Tween (0.05%, PBST), washed twice with PBST, and dried. The microwell array was held in contact with the glass slide under compression in a hybridization chamber (Agilent) and incubated (37°C, 5% CO_2) for 2 hours. After incubation, the glass slide was separated from the microwell array, washed, and labeled with the appropriate fluorescent antibodies, as described previously (40). The printed microarrays were imaged using a GenePix 4200 AL scanner (Molecular Devices).

Data analysis. A custom script was used to identify cells, based on their fluorescence profiles, in the individual wells of the microwell array, as described previously (27). Analysis of the initial set of microscope images (t = 0 hours; t_0) was used to determine the subset of wells containing one live target cell (identified by CellTracker Red; red) and no dead cells (identified by SYTOX; green). Analysis of the second set of microscope images (t = 4 hours [T cell clones] or t = 6 hours [primary $CD8^+$ T cells]; t_{end}) was used to independently determine wells containing 1 target cell (red). An integrity check (database query) was employed to identify wells that contained a single live target at t_0 and a single target at t_{end} ($Wells_{T1}$). The number of effector T cells in wells was determined using calcein violet staining at t_{end} ($Wells_{E1}$, calcein violet positive

and CellTracker Red negative). A second database query was employed to filter $Wells_{T1}$ by $Wells_{E1}$ to identify all wells containing effectors coincubated with single targets ($Wells_{E1T1}$). (For samples with primary $CD8^+$ T cells, we allowed the number of effectors to vary from 1 to 5 as indicated in Results.) These wells were then scored to identify those where the target was also dead at t_{end} (red and green positive; $Wells_{E1T1D}$). Since the arrays of microwells also contained a number of wells containing a single target and no effectors, we performed a similar analysis to identify $Wells_{E0T1}$ and $Wells_{E0T1D}$. These wells made it possible to assess the frequency of nonspecific, spontaneous lysis for each sample ($Wells_{E0T1D}/Wells_{E0T1}$). Background-corrected, effector-mediated lysis frequency was then calculated as ([$Wells_{E1T1D}/Wells_{E1T1}$] – [$Wells_{E0T1D}/Wells_{E0T1}$]). Analysis of the printed microarray was performed as described before (40). Briefly, the images of the printed microarrays were analyzed using GenePix (version 6.0) to extract the fluorescence intensities associated with each element in the array. Data were filtered to exclude elements with saturated pixels or high degrees of covariance (>100). The data for each element in the array were registered with the data on cytolytic activity according to each well's assigned unique identifier.

Generation of T cell clones. $CD8^+$ T cells that mediated the lysis of target cells were retrieved using an automated micromanipulator (CellCelector, AVISO GmbH) (41) and incubated with 10^5 irradiated allogeneic PBMCs in R10 medium containing 50 U/ml IL-2 and incubated at 37°C (5% CO_2) for 30 days (42). Epitope specificity of the generated $CD8^+$ T cell clones was confirmed using MHC class I tetramer staining specific for HLA-B*27-KK10.

ELISpot assay. ELISpot assays were performed to measure antigen-specific release of IFN-γ as described previously, using optimally defined HIV epitopes (43). To calculate the number of specific spot-forming cells (SFCs), the number of spots in the negative control wells was subtracted from the counted number of spots in each well. Negative controls exhibited a maximum of 30 SFCs per 10^6 input cells.

Flow-cytometric detection of antigen-specific $CD8^+$ T cells and assessment of their maturation phenotype. MHC class I tetramer staining was carried out as described previously (44). Briefly, frozen PBMCs were incubated with MHC class I tetramers and then stained with surface antibodies (CD3, CD8, CD27, CD45RA), fixed, and measured on an LSR II flow cytometer (BD). Analysis of the distribution of tetramer-positive cells and their maturation phenotypes was performed using FlowJo 8.8.6 (Tree Star Inc.).

Viral inhibition assay. Inhibition of viral replication by HIV epitope–specific $CD8^+$ T cell clones or bulk $CD8^+$ T cells was assessed in a previously established assay system (33, 45). HLA-matched $CD4^+$ lymphocytes were infected with the HIV-1 isolate JRCSF at an MOI of 0.01. To assess inhibition, $CD8^+$ T cell clones or bulk $CD8^+$ T cells, as indicated, were added at a ratio of 1:1 and incubated for 7 days. At 2- to 3-day intervals, p24 antigen was measured in the supernatant of the cocultures by a standard quantitative enzyme-linked immunosorbent assay (PerkinElmer). All assays were performed in duplicate. Log inhibition units were calculated by subtracting ([$\log_{10}$] p24 with $CD8^+$ T cells) values from ([$\log_{10}$] p24 without $CD8^+$ T cells) values at each time point.

Cytotoxicity assay. B cells (from the same EBV-transformed B cell line used for the microwell assays) were preincubated with 10 μg Gag-KK10 peptide and labeled with 50 μCi $^{51}CrO_4$ (PerkinElmer) for 60 minutes. Cytolytic activity was determined by coincubating target cells and the $CD8^+$ T cell clone 501 at E/T ratios of 5:1, 2.5:1, and 1:1 at 37°C for 2 and 4 hours. All assays were performed in duplicate. Supernatants were harvested and counted on a Cobra Gamma Counter (Packard), and percent lysis was determined according to the formula 100% × ([experimental release – spontaneous release]/[maximum release – spontaneous release]). Maximum release was determined by lysis of targets in 5% Triton. Spontaneous release was less than 12% of maximal release for all reported assays.

TCR α and β chain sequencing. mRNA was extracted from KK10 tetramer-positive $CD8^+$ T cells using the RNeasy Mini Kit (QIAGEN). RACE-Ready cDNA was generated using the SMARTer RACE cDNA Amplification Kit (Clontech). Anchored RT-PCR was then performed using a modified version of the SMARTer (switching mechanism at 5′ end of RNA transcript) procedure and a TCR α or β chain constant region 3′-primer to obtain PCR products containing the Vα or Vβ chain in addition to the CDR3 region, the Jα/β region, and the beginning of the Cα/β region. In short, reverse transcription was carried out at 42°C for 90 minutes with primers provided for the 5′-RACE reaction in a SMART-RACE PCR kit (BD). First- and second-round PCR was then performed using a universal 5′-end primer (5′-CTAATACGACTCACTATAGGGC-3′) and nested gene-specific 3′-end primers annealing to the constant region of the TCR α or β chain (Cα outer: GTCCATAGACCTCATGTCTAGCACAG; Cα inner: ATACACATCAGAATCCTTACTTTG; Cβ outer: 5′-TGTGGCCAGGCACACCAGTGTGGCC-3′; Cβ inner: 5′-GGTGTGGGAGATC-TCTGCTTCTGA-3′). The PCR product was ligated into the TOPO TA cloning vector (Invitrogen) and used to transform *Escherichia coli* (Mach1, Invitrogen). Plasmid DNA was isolated by QIAprep Spin Miniprep Kit (QIAGEN) from selected colonies and sequenced by M13F or M13R primers on an ABI 3100 PRISM automated sequencer. Sequences were edited and aligned using Sequencher (Gene Codes Corp.) and Se-Al (University of Oxford, http://tree.bio.ed.ac.uk/software/seal/) and compared with the human TCR genes database (http://imgt.org/). The TCR Vα/β chain classification system used is that of the international ImMunoGeneTics database (IMGT) (46).

Statistics. Each experiment was tested to verify that the number of cytolytic events scored in wells containing effectors was significantly ($P < 0.05$) greater than the spontaneous lysis observed. A standard, 2-tailed Student's *t* test was used to compare $Wells_{E1T1D}/Wells_{E1T1}$ with $Wells_{E0T1D}/Wells_{E0T1}$. Data clustering and visualization as heatmaps were performed using GenePattern (unsupervised hierarchical clustering: Euclidean distance, complete linkages) (47). The open-source statistics software R was used to estimate the Pearson's product-moment correlation between cytolysis and IFN-γ secretion, and the 95% CI (48). For subjects with KK10-specific $CD8^+$ T cell responses, a subset of the data compiled for all wells with 1–5 effectors and 1 target was generated that included all wells that showed either death of the target at t_{end} or release of IFN-γ. These data were then resampled a fixed number of times (i.e., 50,000), allowing replacement, to select samples of a size equal to the sum of the number of IFN-γ^+ wells and expected number of wells with antigen-specific cytolytic activity (based on the background-corrected frequency of effector-mediated lysis scored). A correlation coefficient (*r*) between cytolysis and IFN-γ secretion was calculated for each sample drawn; these calculated values were used to estimate a mean and 95% CI for the sample. An additional resampling analysis was performed to estimate the probability that the dual function events (IFN-γ secretion and cytolysis) observed in the experiment were due to random overlap of IFN-γ secretion and spontaneous target death. Samples of a size equal to the expected number of spontaneous target death events were drawn from the total set of data from wells with 1–5 effectors and a single target $M = 50{,}000$ times, and the number of IFN-γ^+ wells in each draw was recorded. The number of draws resulting in a number of IFN-γ^+ events greater than or equal to the number of IFN-γ^+ events observed in the actual experiment was determined (*m*), and the probability of random overlap was estimated as $P = m/M$. Random overlap probabilities calculated from the hypergeometric distribution were computed using the hypergeometric cumulative distribution function in MATLAB (MathWorks, release 2010b). Two-tailed Fisher's exact tests were performed using the method of summing small *P* values.

Study approval. The Institutional Review Board of Partners Research Management, Massachusetts General Hospital, and the Committee on the Use of Humans as Experimental Subjects, Massachusetts Institute of Technology, approved the protocols, and all subjects gave written informed consent.

Acknowledgments

The authors thank T.M. Gierahn and M.H. Foley for helpful discussions and J. Choi and M.H. Foley for technical assistance. This research was supported by grants from the Susan and Phillip T. Ragon Foundation, the W.M. Keck Foundation, the Charles A. Dana Foundation, the Ragon Institute of MGH, MIT, and Harvard, the Mark and Lisa Schwartz Foundation, and the Collaboration for AIDS Vaccine Discovery of the Bill and Melinda Gates Foundation. Y.J. Yamanaka was supported in part by a fellowship from the National Science Foundation. A.O. Ogunniyi was supported in part by the NIH (NIGMS 5T32GM008334). J.C. Love is a Latham Family Career Development Professor.

Received for publication April 22, 2011, and accepted in revised form August 10, 2011.

Address correspondence to: J. Christopher Love, Department of Chemical Engineering, Massachusetts Institute of Technology, 77 Massachusetts Ave., Bldg. 76-253, Cambridge, Massachusetts 02139, USA. Phone: 617.324.2300; Fax: 617.258.5042; E-mail: clove@mit.edu.

Navin Varadarajan's present address is: Department of Chemical and Biomolecular Engineering, University of Houston, Houston, Texas, USA.

1. Ndhlovu ZM, Oelke M, Schneck JP, Griffin DE. Dynamic regulation of functionally distinct virus-specific T cells. *Proc Natl Acad Sci U S A*. 2010; 107(8):3669–3674.
2. Migueles SA, et al. HIV-specific CD8+ T cell proliferation is coupled to perforin expression and is maintained in nonprogressors. *Nat Immunol*. 2002; 3(11):1061–1068.
3. Zimmerli SC, Harari A, Cellerai C, Vallelian F, Bart P-A, Pantaleo G. HIV-1-specific IFN-gamma/IL-2-secreting CD8 T cells support CD4-independent proliferation of HIV-1-specific CD8 T cells. *Proc Natl Acad Sci U S A*. 2005;102(20):7239–7244.
4. Migueles SA, et al. Lytic granule loading of CD8+ T cells is required for HIV-infected cell elimination associated with immune control. *Immunity*. 2008; 29(6):1009–1021.
5. Rutebemberwa A, et al. High-programmed death-1 levels on hepatitis C virus-specific T cells during acute infection are associated with viral persistence and require preservation of cognate antigen during chronic infection. *J Immunol*. 2008; 181(12):8215–8225.
6. Zhang D, et al. Most antiviral CD8 T cells during chronic viral infection do not express high levels of perforin and are not directly cytotoxic. *Blood*. 2003; 101(1):226–235.
7. Betts MR, et al. Sensitive and viable identification of antigen–specific CD8+ T cells by a flow cytometric assay for degranulation. *J Immunol Methods*. 2003; 281(1–2):65–78.
8. Lichterfeld M, et al. Loss of HIV-1-specific CD8+ T cell proliferation after acute HIV-1 infection and restoration by vaccine-induced HIV-1-specific CD4+ T cells. *J Exp Med*. 2004;200(6):701–712.
9. Betts MR, et al. HIV nonprogressors preferentially maintain highly functional HIV-specific CD8+ T cells. *Blood*. 2006;107(12):4781–4789.
10. Almeida JR, et al. Superior control of HIV-1 replication by CD8+ T cells is reflected by their avidity, polyfunctionality, and clonal turnover. *J Exp Med*. 2007; 204(10):2473–2485.
11. Hersperger AR, et al. Perforin expression directly ex vivo by HIV-specific CD8 T-cells is a correlate of HIV elite control. *PLoS Pathog*. 2010;6(5):e1000917.
12. Goulder PJR, Watkins DI. Impact of MHC class I diversity on immune control of immunodeficiency virus replication. *Nat Rev Immunol*. 2008; 8(8):619–630.
13. Appay V, Douek DC, Price DA. CD8+ T cell efficacy in vaccination and disease. *Nat Med*. 2008; 14(6):623–628.
14. D'Souza MP, Altfeld M. Measuring HIV-1-specific T cell immunity: how valid are current assays? *J Infect Dis*. 2008;197(3):337–339.
15. Streeck H, Frahm N, Walker B. The role of IFN-gamma Elispot assay in HIV vaccine research. *Nat Protoc*. 2009;4(4):461–469.
16. Snyder JE, Bowers WJ, Livingstone AM, Lee FE-H, Federoff HJ, Mosmann TR. Measuring the frequency of mouse and human cytotoxic T cells by the Lysispot assay: independent regulation of cytokine secretion and short-term killing. *Nat Med*. 2003; 9(2):231–235.
17. Lamoreaux L, Roederer M, Koup R. Intracellular cytokine optimization and standard operating procedure. *Nat Protoc*. 2006;1(3):1507–1516.
18. Seder RA, Darrah PA, Roederer M. T-cell quality in memory and protection: implications for vaccine design. *Nat Rev Immunol*. 2008;8(4):247–258.
19. Harari A, Enders FB, Cellerai C, Bart PA, Pantaleo G. Distinct profiles of cytotoxic granules in memory CD8 T cells correlate with function, differentiation stage, and antigen exposure. *J Virol*. 2009;83(7):2862–2871.
20. Ratner A, Clark WR. Role of TNF-alpha in CD8+ cytotoxic T lymphocyte-mediated lysis. *J Immunol*. 1993; 150(10):4303–4314.
21. Makedonas G, Betts MR. Living in a house of cards: re-evaluating CD8+ T-cell immune correlates against HIV. *Immunol Rev*. 2011;239(1):109–124.
22. Neitzel H. A routine method for the establishment of permanent growing lymphoblastoid cell lines. *Human Genetics*. 1986;73(4):320–326.
23. Johnson VA, Walker BD, Barlow MA, Paradis TJ, Chou TC, Hirsch MS. Synergistic inhibition of human immunodeficiency virus type 1 and type 2 replication in vitro by castanospermine and 3′-azido-3′-deoxythymidine. *Antimicrob Agents Chemother*. 1989;33(1):53–57.
24. Champagne P, et al. Skewed maturation of memory HIV-specific CD8 T lymphocytes. *Nature*. 2001; 410(6824):106–111.
25. Fearon DT, Manders P, Wagner SD. Arrested differentiation, the self-renewing memory lymphocyte, and vaccination. *Science*. 2001;293(5528):248–250.
26. Bradshaw EM, et al. Concurrent detection of secreted products from human lymphocytes by microengraving: antigen-reactive antibodies and cytokines. *Clin Immunol*. 2008;129(1):10–18.
27. Han Q, Bradshaw EM, Nilsson B, Hafler DA, Love JC. Multidimensional analysis of the frequencies and rates of cytokine secretion from single cells by quantitative microengraving. *Lab Chip*. 2010;10(11):1391–1400.
28. Almeida JR, et al. Antigen sensitivity is a major determinant of CD8+ T-cell polyfunctionality and HIV-suppressive activity. *Blood*. 2009;113(25):6351–6360.
29. Betts MR, et al. The functional profile of primary human antiviral CD8+ T cell effector activity is dictated by cognate peptide concentration. *J Immunol*. 2004;172(10):6407–6417.
30. Study IHC, et al. The major genetic determinants of HIV-1 control affect HLA class I peptide presentation. *Science*. 2010;330(6010):1551–1557.
31. Goulder PJ, et al. Late escape from an immunodominant cytotoxic T-lymphocyte response associated with progression to AIDS. *Nat Med*. 1997;3(2):212–217.
32. Altfeld M, et al. HLA Alleles Associated with Delayed Progression to AIDS Contribute Strongly to the Initial CD8(+) T Cell Response against HIV-1. *PLoS Med*. 2006;3(10):e403.
33. Chen H, et al. Differential neutralization of human immunodeficiency virus (HIV) replication in autologous CD4 T cells by HIV-specific cytotoxic T lymphocytes. *J Virol*. 2009;83(7):3138–3149.
34. Schneidewind A, et al. Transmission and long-term stability of compensated CD8 escape mutations. *J Virol*. 2009;83(8):3993–3997.
35. Sad S, Kägi D, Mosmann TR. Perforin and Fas killing by CD8+ T cells limits their cytokine synthesis and proliferation. *J Exp Med*. 1996;184(4):1543–1547.
36. Tan LC, et al. A re-evaluation of the frequency of CD8+ T cells specific for EBV in healthy virus carriers. *J Immunol*. 1999;162(3):1827–1835.
37. Goepfert PA, et al. A significant number of human immunodeficiency virus epitope-specific cytotoxic T lymphocytes detected by tetramer binding do not produce gamma interferon. *J Virol*. 2000; 74(21):10249–10255.
38. Schaubert KL, et al. Availability of a diversely avid CD8+ T cell repertoire specific for the subdominant HLA-A2-restricted HIV-1 Gag p2419-27 epitope. *J Immunol*. 2007;178(12):7756–7766.
39. Zloza A, Schenkel JM, Tenorio AR, Martinson JA, Jeziorczak PM, Al-Harthi L. Potent HIV-specific responses are enriched in a unique subset of CD8+ T cells that coexpresses CD4 on its surface. *Blood*. 2009;114(18):3841–3853.
40. Ogunniyi AO, Story CM, Papa E, Guillen E, Love JC. Screening individual hybridomas by microengraving to discover monoclonal antibodies. *Nat Protoc*. 2009;4(5):767–782.
41. Choi JH, et al. Development and optimization of a process for automated recovery of single cells identified by microengraving. *Biotechnol Prog*. 2010; 26(3):888–895.
42. Walker BD, et al. Long-term culture and fine specificity of human cytotoxic T-lymphocyte clones reactive with human immunodeficiency virus type 1. *Proc Natl Acad Sci U S A*. 1989;86(23):9514–9518.
43. Addo MM, et al. Comprehensive epitope analysis of human immunodeficiency virus type 1 (HIV-1)-specific T-cell responses directed against the entire expressed HIV-1 genome demonstrate broadly directed responses, but no correlation to viral load. *J Virol*. 2003;77(3):2081–2092.
44. Streeck H, et al. Antigen load and viral sequence diversification determine the functional profile of HIV-1-specific CD8+ T cells. *PLoS Med*. 2008;5(5):e100.
45. Julg B, et al. Enhanced anti-HIV functional activity associated with Gag-specific CD8 T-cell responses. *J Virol*. 2010;84(11):5540–5549.
46. Lefranc M-P, et al. IMGT unique numbering for immunoglobulin and T cell receptor variable domains and Ig superfamily V-like domains. *Dev Comp Immunol*. 2003;27(1):55–77.
47. Reich M, Liefeld T, Gould J, Lerner J, Tamayo P, Mesirov JP. GenePattern 2.0. *Nat Genet*. 2006; 38(5):500–501.
48. R Development Core Team. *R: A Language and Environment for Statistical Computing*. Vienna, Austria: R Foundation for Statistical Computing; 2008.